



Short Note

(E)-4-(3-(3-(4-Methoxyphenyl)acryloyl)phenoxy)butyl 2-Hydroxybenzoate

Ihsan Ikhtiarudin ^{1,*}, Rahma Dona ¹, Neni Frimayanti ¹, Rahayu Utami ¹, Emma Susanti ¹, Mentari Mentari ¹, Nurmaida Nurmaida ¹, Nesa Agistia ¹, Noval Herfindo ^{2,3}  and Adel Zamri ³ 

- ¹ Department of Pharmacy, Sekolah Tinggi Ilmu Farmasi (STIFAR) Riau, Pekanbaru 28293, Indonesia; rahmadona@stifar-riau.ac.id (R.D.); nenifrimayanti@gmail.com (N.F.); rahayuutami@stifar-riau.ac.id (R.U.); emmasusanti@stifar-riau.ac.id (E.S.); 15mentari@stifar-riau.ac.id (M.M.); nrmaida12@gmail.com (N.N.); nesaagistia@stifar-riau.ac.id (N.A.)
- ² Department of Biomedical Engineering, Faculty of Engineering, King Mongkut's Institute of Technology Ladkrabang, Bangkok 10520, Thailand; novalherfindo@gmail.com
- ³ Department of Chemistry, Faculty of Mathematics and Natural Sciences, Universitas Riau, Pekanbaru 28293, Indonesia; adel.zamri@lecturer.unri.ac.id
- * Correspondence: ihsanikhtiarudin@stifar-riau.ac.id

Abstract: A new hybrid compound of chalcone-salicylate (title compound) has been successfully synthesized using a linker mode approach under reflux condition. The structure of the title compound has been established by spectroscopic analysis including UV-Vis, FT-IR, HRMS, 1D, and 2D NMR. Then, computational approach was also applied in this study through molecular docking and MD simulation to explore its potency against breast cancer. The results of the molecular docking study showed that the title compound exhibited more negative value of binding free energy (−8.15 kcal/mol) than tamoxifen (−7.00 kcal/mol). In addition, no striking change in the positioning of the interacting residues was recorded before and after the MD simulations. Based on the studies, it can be predicted that the title compound has a cytotoxic activity potency against breast cancer through ER α inhibition and it presumably can be developed as anticancer agent candidate.

Keywords: chalcone; salicylic acid; hybrid compound; molecular hybridization; chalcone-salicylate; in silico study; computational approaches; molecular docking; MD simulation



Citation: Ikhtiarudin, I.; Dona, R.; Frimayanti, N.; Utami, R.; Susanti, E.; Mentari, M.; Nurmaida, N.; Agistia, N.; Herfindo, N.; Zamri, A. (E)-4-(3-(3-(4-Methoxyphenyl)acryloyl)phenoxy)butyl 2-Hydroxybenzoate. *Molbank* **2021**, *2021*, M1195. <https://doi.org/10.3390/M1195>

Academic Editor: Fawaz Aldabbagh

Received: 22 February 2021

Accepted: 2 March 2021

Published: 9 March 2021

Publisher's Note: MDPI stays neutral with regard to jurisdictional claims in published maps and institutional affiliations.



Copyright: © 2021 by the authors. Licensee MDPI, Basel, Switzerland. This article is an open access article distributed under the terms and conditions of the Creative Commons Attribution (CC BY) license (<https://creativecommons.org/licenses/by/4.0/>).

1. Introduction

Chalcones (1,3-diphenyl-prop-2-en-1-ones) are natural products that are found in several plant species and they have been reported for broad spectrum of biological activities. Their analogues and derivatives have been widely synthesized to explore their potential uses [1–3], especially in anticancer drug discovery researches [4]. Some researchers have reported that several hydroxylated and methoxylated chalcones exhibited potent cytotoxic activity against the MCF-7 cell line [4,5]. Besides chalcones, some salicylic acid derivatives have also been reported as potent cytotoxic agents against several cancer cell lines, including MCF-7 [6]. Based on the report, the IC₅₀ values of some tested compounds are close to the IC₅₀ of 5-fluorouracil. In addition, some hybrid compounds such as β -carboline-salicylates have also exhibited potent cytotoxic activity against various cell lines [7]. A hybrid of 4-farnesyltiosalicylate-salicylate also possessed the higher cytotoxic activity against MCF-7 cell line than a withdrawn drug, sorafenib (Nexavar) [8]. Therefore, designing and synthesizing a new compound through the molecular hybridization approach is an interesting option in order to search for new anticancer agent candidates. Some workers have reported that this approach has been proven to be an effective way to develop new multifunctional compounds from hybridization or conjugation of two or more molecules that are expected to have a better biological activity than their parent compounds [9].

In this work, we report the synthesis of a new hybrid compound, (E)-4-(3-(3-(4-methoxyphenyl)acryloyl)phenoxy)butyl 2-hydroxybenzoate (title compound) using a

linker mode approach. The potency of cytotoxic activity of the title compound against breast cancer was studied *in silico* using computational approaches (molecular docking and MD simulation).

2. Results and Discussions

2.1. Synthesis of Title Compound (2)

In this work, we have successfully synthesized a new hybrid compound of chalcone-salicylate (2) by combining both structures of a substituted chalcone analog (1) and salicylic acid, using linker mode approach [9]. The linker was used because the steric hindrance from both molecules that will be linked usually became a problem in molecular hybridization [10,11]. Application of a linker is a way to minimize the steric hindrance [11,12]. In this work, we used the 1,4-dibromobutane as a linker. The reaction was performed under reflux condition in acetonitrile with the presence of potassium carbonate as catalyst, as described in Figure 1.

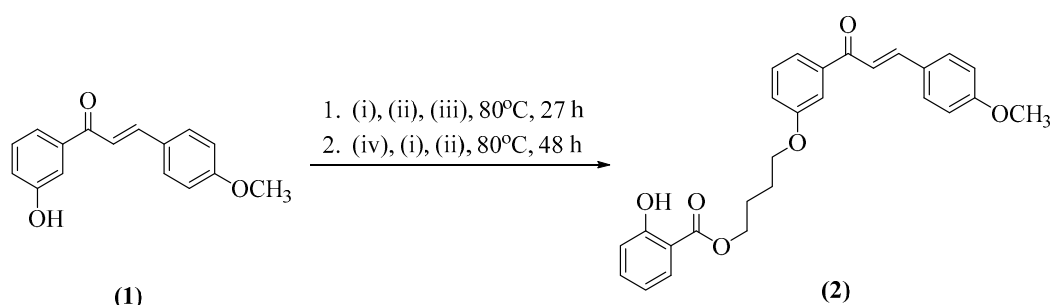


Figure 1. The synthesis route of title compound (2) under reflux condition, (i) ACN, (ii) K_2CO_3 , (iii) $(CH_2)_4Br_2$, (iv) salicylic acid.

The title compound in pure form was obtained as clear yellow crystal in 33.13% yield, with melting point of 55–57 °C. The purity of the synthesized product was determined by TLC and HPLC analysis, as shown in Supplementary Material. The structure of the title compound has been confirmed by spectroscopic analysis including UV, FT-IR, HRMS, 1D, and 2D NMR. The FT-IR analysis was performed to ensure that the functional groups present in the synthesized compound match the functional groups present in target molecule. Based on the FT-IR spectra, the title compound showed the broad absorption band at 3112 cm^{-1} . This absorbance showed the presence of hydroxyl (O-H group) in *ortho* position bonded to carbonyl group of salicylate through intramolecular hydrogen bond formation. The absorption bands at 3076 cm^{-1} and $1594\text{--}1449\text{ cm}^{-1}$ showed the presence of aromatic C-H and C=C bonds in three aromatic rings of title compound, while the absorption band at 2953 and 2868 cm^{-1} showed the symmetrical and asymmetrical stretching of C-H in methoxy group of title compound. The presence of carbonyl group of ester and ketone is shown by the two vibration bands at 1672 and 1657 cm^{-1} , respectively. In addition, the absorption bands around $1298\text{--}1028\text{ cm}^{-1}$ showed the presence of C-O bonds in ether and ester groups of title compound. The other types of vibrations can be seen in Supplementary Material. In addition, the HRMS analysis was also performed to determine the molecular weight of the synthesized compound. Based on the mass spectral analysis, the synthesized compound has a molecular weight corresponding to the molecular weight of the title compound. The molecular ion peak $[M + Na^+]$ of the title compound is found at m/z 469.1616 with intensity of 100%, while the calculated mass is 469.1627, as shown in Supplementary Material.

The 1D NMR spectra was measured to confirm the structure of the title compound based on the number and chemical environment of protons and carbons. The 1H NMR spectra of the title compound in $CDCl_3$ showed a singlet peak (1H) at δ 10.82 ppm due to the presence of hydroxyl group in the aromatic ring of the salicylate moiety. In addition, the aromatic proton signals around δ 7.84–6.87 ppm (12 H) were assigned as aromatic protons in three substituted aromatic rings of the title compound, whereas the signals around

δ 4.46–2.01 ppm (11 H) were also assigned as aliphatic protons. Then, the two doublet signals at δ 7.80 ppm (1H) and 7.40 ppm (1H) were assigned as H β and H α protons, respectively. Based on the calculation, the coupling constants (J) of both doublet signals are 15.5 Hz. The coupling constants showed that both protons are in *trans* (*E*) position. Based on the interpretation of ^1H NMR spectral data, the synthesized compound has 26 protons, corresponds to the number of protons present in the expected structure. The presence of a methoxy group was observed by the appearance of a singlet signal at δ 3.87 ppm. Then, the appearance of two triplet signals and a multiplet signal in the aliphatic proton region were assigned as four methylene groups ($-\text{CH}_2-$)₄ in the title compound, as described clearly in Supplementary Material and Table 1.

Table 1. The 1D and 2D NMR spectra interpretations of the title compound.

Carbons	^1H NMR δ (ppm), J (Hz)	^{13}C NMR δ (ppm)	^1H - ^1H COSY	Important ^1H - ^{13}C HMBC
1	-	112.46	-	-
2	10.82 (s, 1H, OH)	161.67	-	112.46 (C1), 161.67(C2), 117.58 (C3)
3	6.99 (d, 1H, $J = 8.5$ Hz)	117.58	4	-
4	7.46 (dt, 1H, $J_1 = 8$ Hz, $J_2 = 1.5$ Hz)	135.67	3, 5	-
5	6.87 (t, 1H, $J = 7.5$ Hz)	119.14	4, 6	-
6	7.84 (dd, 1H, $J_1 = 8$ Hz, $J_2 = 1.5$ Hz)	129.82	5	-
C=O ester	-	170.15	-	-
1'	4.46 (t, 2H, $J = 5.5$ Hz)	64.98	2'	170.15 (C=O ester)
2'	2.01 (m, 2H)	25.44	1'	-
3'	2.01 (m, 2H)	25.90	4'	-
4'	4.13 (t, 2H, $J = 5.5$ Hz)	67.42	3'	159.13 (C3')
1''	-	159.13	-	-
2''	7.55 (s, 1H)	113.47	3''	190.19 (C=O ketone)
3''	-	139.92	-	-
4''	7.60 (d, 1H, $J = 6$ Hz)	121.00	5''	190.19 (C=O ketone)
5''	7.41 (t, 1H, $J = 8$ Hz)	119.76	4'' 6''	139.92 (C3''), 159.13 (C1'')
6''	7.12 (dd, 1H, $J_1 = 8$ Hz, $J_2 = 2$ Hz)	119.41	5'' 2''	-
C=O ketone	-	190.19	-	-
C α	7.40 (d, 1H, $J = 15.5$ Hz)	129.54	β	190.19 (C=O ketone), 127.60 (C1'''), 130.24 (C2''')
C β	7.80 (d, 1H, $J = 15.5$ Hz)	144.72	α	190.19 (C=O ketone), 139.92 (C3''); 127.60 (C1''')
1'''	-	127.60	-	-
2'''/6'''	7.61 (d, 2H, $J = 8.5$ Hz)	130.24	3'''/5'''	144.72 (C β); 161.70 (C4''')
3'''/5'''	6.95 (d, 2H, $J = 8.5$ Hz);	114.42	2'''/6'''	127.60 (C1''')
4'''	-	161.70	-	-
OCH ₃	3.87 (s, 3H)	55.41	-	161.70 (C4''')

The ^{13}C NMR spectra of the title compound in CDCl_3 showed that two specific signals at δ 190.19 and 170.15 ppm were assigned as carbonyl signals of ketone and ester, respectively. In addition, the carbon signals around δ 161.70–112.46 ppm were assigned as aromatic carbon signals on three aromatic rings of the title compound including three oxyaryl carbons C2 (161.67), C1'' (159.13), and C4''' (161.70). Then, five carbon signals around δ 67.42–25.44 ppm were assigned as aliphatic carbon signals of a methoxy group and four methylene carbons in the title compound, as described in Supplementary Material and Table 1. Based on the interpretation of ^{13}C NMR spectral data, the synthesized compound has 27 carbons, and it is matched with the number of carbon in the expected structure.

The assignments of ^1H and ^{13}C NMR spectra of the title compound were supported by ^1D -TOCSY, ^{13}C -DEPT, COSY, HSQC, and HMBC spectra, as described clearly in Supplementary Material. The ^1H - ^1H correlations in HMBC spectra ensured that the linker is bound to carboxyl group, as depicted in Figure 2. The interpretation result of COSY, HSQC,

and HMBC spectra showed that the ^1H - ^1H and ^1H - ^{13}C correlations in the title compound are matched with the expected structure.

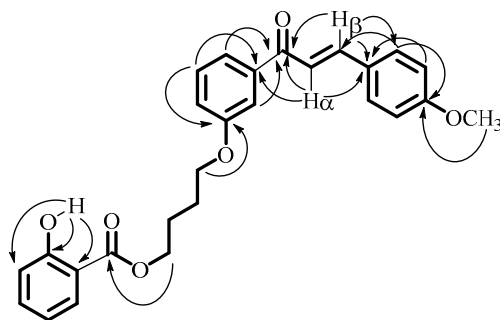


Figure 2. The important ^1H - ^{13}C correlations in the HMBC spectra of the title compound.

2.2. Molecular Docking Study and MD Simulation

The molecular docking study was performed to predict the ability of the title compound to bind with the estrogen receptor. This receptor is classified into two subtypes, ER α and ER β . Both receptors are present in the mammary gland [13]. ER α plays an important role in cell proliferation [14] and pathogenesis of breast cancers [15]. Approximately 75% of breast cancers have positive expression of this specific type of hormonal receptor [16]. Therefore, targeting this receptor is an attractive option for finding a new anticancer agent for breast cancer.

In this work, the molecular docking study was performed for the starting material (chalcone analogue), title compound (hybrid of chalcone-salicylate), and tamoxifen as a reference drug to treat breast cancer. The crystal structure of ER α was downloaded from rcsb.org with PDB ID of 3ERT. This crystal structure is bound to a co-crystallized ligand, 4-OHT, one of the major active metabolites of tamoxifen [17]. The docking study was performed in several steps, as described in the procedure section. After the protein and ligands were prepared, a validation of docking protocol is required to ensure the accuracy of the docking result [18–20]. The validation of docking protocol can be performed by re-docking the co-crystallized ligand (4-OHT) to the prepared receptor. The validation result of docking protocol is presented in Supplementary Material. The result showed that the similarity of binding poses between co-crystallized ligand and re-docking ligand is 81.48% with RMSD value less than 2. These results showed that the docking protocol was valid. The 3D and 2D binding poses of re-docked ligand (4-OHT) is depicted in Supplementary Material and the comparison of binding poses of co-crystallized (yellow color) and re-docked ligand (atomic coloring) are depicted in Figure 3. Based on the figure, we can observe that they are superimposed.

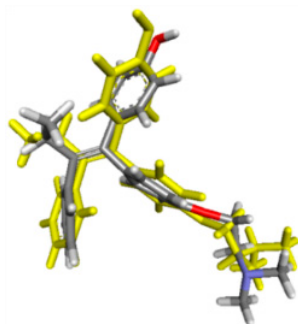


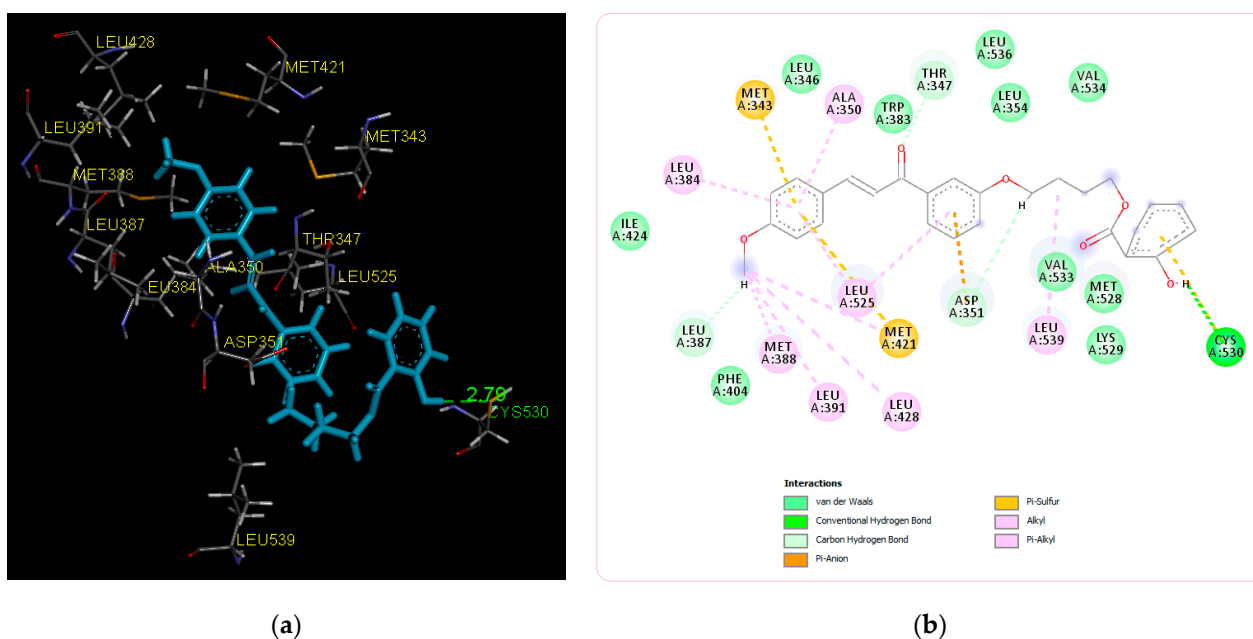
Figure 3. Binding poses of 4-OHT as co-crystallized ligand (yellow) and re-docked native ligand (atomic coloring).

Based on the docking result, the chalcone analogue, title compound, and tamoxifen show similar interactions to 4-OHT. Based on the Table 2, we observed that the title compound had more negative binding free energy (-8.15 kcal/mol) when compared to the chalcone analogue (-6.32 kcal/mol) and tamoxifen (-7.00 kcal/mol). More negative binding free energy indicates that the title compound is more easily bound to the ER α [18]. In addition, we also observed that the binding free energy of the title compound was very close with the binding free energy of 4-OHT as native ligand (-9.02 kcal/mol).

Table 2. The docking result for ER α (defined in Appendix A).

Compounds	ΔG (kcal/mol)	Interactions with Amino Acid Residues		
		H Bond	van der Walls	Other Hydrophobic Interactions
Chalcone analogue	-6.32	Glu353	Arg394, Leu428, Met388, Ile424, Met421, Gly521, Gly420, Glu419, Thr347	His524, Leu525, Leu384, Met343, Leu349, Phe404, Leu346, Leu391, Leu387, Ala350
Title Compound	-8.15	Cys530	Ile424, Phe404, Val533, Met528, Lys529, Val534, Leu354, Leu536, Trp383, Leu346	Leu387, Asp351, Thr347, Leu384, Met343, Ala350, Met388, Leu391, Leu428, Leu525, Met421, Leu539
Tamoxifen	-7.00	-	Arg394, Glu353, Met517, Met388, Ile424, Gly521, Lys520, Gly521, His524, Gly420, Leu354, Met528, Trp383, Thr347, Leu536, Leu428, Phe404	Leu525, Asp351, Leu384, Met421, Met343, Leu349, Leu346, Leu387, Leu391, Ala350
4-OHT	-9.02	Glu353	Glu419, Ile424, Gly420, His524, Gly521, Met522, Arg394, Phe404, Thr347, Lys529, Trp383, Leu536, Leu354, Leu539	Asp351, Leu525, Met421, Leu428, Met388, Leu391, Met343, Ala350, Leu384, Leu387, Leu346, Leu349

The chalcone analogue is able to form one hydrogen bond to Glu353 residue in the active site of ER α . This interaction was also observed between 4-OHT and ER α . However, 4-OHT has more van der Walls and other hydrophobic interactions that might cause 4-OHT to have more negative value of binding free energy than chalcone analogue. In addition, the title compound is also able to form hydrogen bond, but with different amino acid residue (Cys530). This interaction is not observed for other docked compounds. However, there are 18 similar interactions between the title compound and tamoxifen, and there are 19 similar interactions between the title compound and 4-OHT, as depicted in Table 2. The 3D and 2D visualizations of the docking result of the title compound are depicted in Figure 4 and more complete visualizations of all docked compounds are depicted in Supplementary Material. Based on the figure in Supplementary Material, we observed that the chalcone analogue, title compound, and tamoxifen are bound to ER α with similar binding poses. Then, based on Figure 5, we can observe that they are superimposed.



(a)

(b)

Figure 4. The binding modes of title compound to ER α using Discovery Studio 2020 Client, (a) 3D visualization, and (b) 2D visualization.

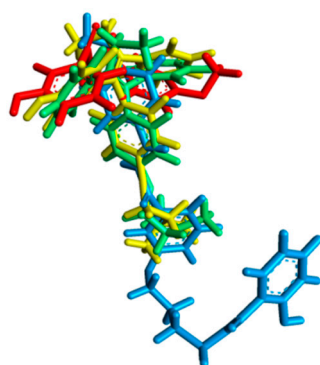


Figure 5. Superimposition of docked compounds, chalcone analogue (red), title compound (blue), tamoxifen (green), and 4-OHT (yellow).

MD simulation was also performed to observe the stability of the protein–ligand complex. This simulation treats both protein and ligand as flexible entities, involves the binding and breaking of the hydrogen bonds and other interactions in the protein–ligand complex caused by the continuous motion of the molecules, and also computing movements as a function of time [21]. This simulation can aid us to ensure whether the interactions between the compound and protein were still maintained or not during the simulation [22–24]. The MD simulation result showed that the hydrogen bond between hydroxyl group of title compound and Cys530 (2.79 Å) was broken, caused by conformational changing. However, most of interactions between the title compound and ER α are still maintained, and amazingly, after MD simulation, two new hydrogen bonds are formed, between the hydroxyl group of the title compound with Asp351 (1.66 Å) and between ketone carbonyl group with Thr347 (2.02 Å). Based on the literature [20], the hydrophilic interactions with both residues are playing important role in antagonist activity of 4-OHT to ER α . The MD simulation results are presented in Table 3 and depicted in Supplementary Material. A comparison of binding poses of the title compound before and after MD simulation is depicted in Figure 6. Notably, no striking change in the positioning of the interacting residues was recorded before and after the MD simulations. In addition, they are still superimposed.

Table 3. Comparison of interactions of the title compound with amino acid residues before and after MD simulation.

	Amino Acid Residues		
	H Bond	van der Waals	Other Hydrophobic Interactions
Before MD simulation	Cys530	Ile424, Phe404, Val533, Met528, Lys529, Val534, Leu354, Leu536, Trp383, Leu346	Leu387, Asp351, Thr347, Leu384, Met343, Ala350, Met388, Leu391, Leu428, Leu525, Met421, Leu539
After MD simulation	Asp351, Thr347	Met388, Gly521, Leu384, Leu525, Leu536, Ile358, Leu540, Leu539, Met543, Asn532, Gly420	His524, Pro535, Ile424, Met421, Leu346, Ala350, Leu354, Val534, Lys529, Trp383

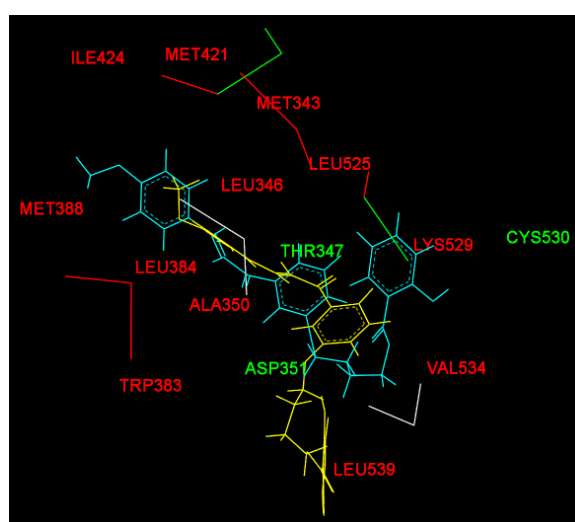


Figure 6. The 3D visualization of superimposition of binding poses of the title compound before and after MD simulation. Binding pose before MD simulation is presented in blue and after MD is presented in yellow. The amino acid residue with hydrogen bond is presented in green and the other maintained interactions during MD simulation are presented in red.

3. Materials and Methods

3.1. Materials

The materials used in this work are a chalcone analogue from our previously work [3], recrystallized salicylic acid (Brataco, Pekabaru, Indonesia), 1,4-dibromobutane 99% (Merck, Darmstadt, Germany), potassium carbonate for analysis (Merck, Darmstadt, Germany), and some of organic solvents, such as acetonitrile for analysis, absolute ethanol, *n*-hexane, ethyl acetate, and dichloromethane were purchased from Merck, Darmstadt, Germany.

3.2. Instrumentations

The instruments used in synthesis, purification, and structure characterization of the title compound are a set of reflux apparatus, vacuum rotary evaporator (Buchi[®], Flawil, Switzerland), column chromatography (Pyrex[®], France), UV Lamp 254/366 nm (Camag[®], Muttenz, Swiss), Stuart Melting Point Apparatus (SMP-11, Staffordshire, UK), HPLC (Shimadzu[®] LC solution, Japan), UV-Vis spectrophotometer (Genesys[™] 10S, Waltham, MA, USA), FT-IR spectrophotometer (Shimadzu[®] FT-IR Prestige-21, Kyoto City, Japan), HRMS (Waters ESI-TOF ES+, Singapore), and NMR spectrometer (Agilent, 500 MHz for ¹H NMR and 125 MHz for ¹³C NMR, Santa Clara, CA, USA). The in silico study was performed by MOE 2019.0101 software package (Chemical Computing Group, Tokyo, Japan).

3.3. Methods

3.3.1. Synthesis of (*E*)-4-(3-(3-(4-Methoxyphenyl)acryloyl)phenoxy)butyl 2-Hydroxybenzoate

As much as 9 mmol (1.9431 g) of 1,4-dibromobutane was diluted in 50 mL of acetonitrile in a round bottom flask (mixture 1), 3 mmol (0.762 g) of chalcone analogue was dissolved in 15 mL acetonitrile (mixture 2), and 6 mmol (0.8292 g) of potassium carbonate was added into mixture 2. Then, the mixture 2 was poured into mixture 1. The reaction mixture was refluxed and stirred on the oil bath at 80–85 °C until the reaction was completed (27 h). After the reaction was completed (observed by TLC analysis), the intermediate solution was used immediately without further purification. A mixture of 6 mmol (0.828 g) of salicylic acid and 4 mmol (0.5528 g) of potassium carbonate in 7.5 mL acetonitrile was added to the intermediate solution and then refluxed and stirred at 80 °C until the reaction was completed (48 h). After the reaction was completed (observed by TLC analysis), the mixture of the product was poured in a separatory funnel and washed by distilled water (3 × 15 mL). Then, the solvent was evaporated using vacuum rotary evaporator to afford the crude product. This crude product was purified through a SiO₂ column chromatography with a mixture of *n*-hexane and ethyl acetate (8:2) as mobile phase to get pure product of chalcone-salicylate. The purity of hybrid compound was confirmed by TLC and HPLC analysis. Then, the structure of hybrid compound was confirmed by spectroscopic analysis including FT-IR, HRMS, 1D NMR (¹H NMR, ¹³C NMR, DEPT-135, 1D TOCSY), and 2D NMR (COSY, HSQC, HMBC).

The title compound was obtained as a clear yellow crystal in 33.13% yield, mp. 55–57 °C. UV spectra (in ethanol), λ_{max} (nm): 292 nm. FT-IR spectra (KBr) (cm⁻¹): 3112, 3076, 2953, 2868, 1672, 1657, 1594, 1572, 1511, 1450, 1298, 1253, 1213, 1177, 1028. HRMS spectra, molecular ion peak [M + Na⁺] was found at *m/z* 469.1616, while calculated mass was 469.1627, as shown in Supplementary Material. NMR (CDCl₃, 500 MHz), δ (ppm): 10.82 (s, 1H), 7.84 (dd, 1H, *J*₁ = 8 Hz, *J*₂ = 1.5 Hz), 7.80 (d, 1H, *J* = 15.5 Hz), 7.61 (d, 2H, *J* = 8.5 Hz), 7.60 (d, 1H, *J* = 6 Hz), 7.55 (s, 1H), 7.46 (dt, 1H, *J*₁ = 8.5 Hz, *J*₂ = 1.5 Hz), 7.41 (t, 1H, *J* = 8 Hz), 7.40 (d, 1H, *J* = 15.5), 7.12 (dd, 1H, *J*₁ = 8 Hz, *J*₂ = 2 Hz), 6.99 (d, 1H, *J* = 8.5 Hz), 6.95 (d, 2H, *J* = 8.5 Hz), 6.87 (t, 1H, *J* = 7.5 Hz), 4.46 (t, 2H, *J* = 5.5 Hz), 4.13 (t, 2H, *J* = 5.5 Hz), 3.87 (s, 3H), 2.01 (m, 4H). ¹³C NMR (CDCl₃, 125 MHz), δ (ppm): 190.19, 170.15, 161.70, 161.67, 159.13, 144.72, 139.92, 135.67, 130.24 (2C), 129.82, 129.54, 127.60, 121.00, 119.76, 119.41, 119.14, 117.58, 114.42 (2C), 113.47, 112.46, 67.42, 64.98, 55.41, 25.90, 25.44. The complete 2D NMR spectra of the title compound are shown in Supplementary Material.

3.3.2. Molecular Docking Study

The structure of ligands were drawn using ChemDraw Professional 15.0 and a database of ligand was created using MOE 2019.0101 software package (Chemical Computing Group, Tokyo, Japan). The crystal structure of ERα with PDB ID 3ERT was downloaded from <http://www.rcsb.org> [18–20] and was prepared in Discovery Studio 2020 Client to remove the water, co-crystallized ligand, and then, it was further prepared using MOE to minimize the energy. Before running the docking, the placement and refinement method were set as alpha triangle and rigid receptor, respectively. The placement and refinement scores were set as Afinity dG. Then, the placement and refinement poses were set as 100 and 30, respectively. The other parameters were set as default. The 4-OHT as native ligand was re-docked to the prepared protein to validate this docking protocol. After the protocol was validated, the other ligands were docked with same method. The best poses of docking results were selected based on some parameters such as binding free energy, RMSD, and the similarity of interactions compared to the 4-OHT as native ligand and to tamoxifen as breast cancer drug. The best poses of the docked ligands were presented in 2D and 3D visualization using Discovery Studio 2020 Client.

3.3.3. MD Simulation

The MD simulation was also performed using MOE. Before run the simulation, the algorithm was set as NPA. The start time, checkpoint, and sample time were set as 0, 300, and 0.01, respectively. Then, the forcefield was set as CHARMM27, and the other parameters were set as default. The result of MD simulation was presented in 2D and 3D visualization using Discovery Studio 2020 Client. Then, the protein–ligand interactions before and after MD simulation were compared.

4. Conclusions

In this work, we have successfully synthesized a new hybrid compound of chalcone-salicylate. Based on spectroscopy analysis, the structure of the synthesized compound was matched with the expected structure. The molecular docking and MD simulation results predicted that the title compound has cytotoxic potency against breast cancer through binding with ER α and it presumably can be developed as a new anticancer agent candidate. However, the in vitro and in vivo evaluations are required to ensure its cytotoxic potency.

Supplementary Materials: The following are available online, Figure S1: the clear yellow crystal of the title compound (hybrid compound), Figure S2: TLC chromatogram of hybrid compound (HC) compared to chalcone analog (CA) and salicylic acid (SA) as starting materials under UV lamp, 254 nm. H = *n*-hexane and E = ethyl acetate, Figure S3: the result of TLC analysis of hybrid compound using various mobile phases: (a) *n*-hexane: ethyl acetate (9:1), (b) DCM: *n*-hexane (8:2), (c) D100% = DCM 100%, Figure S4: HPLC chromatogram of hybrid compound, analysis was performed using reverse phase column Shim-Pack VP-ODS (150 \times 4.6 mm) with gradient elution method using water and acetonitrile (HPLC grade) as mobile phase for 20 minutes with flow rate 1 ml/minute, Figure S5: the FT-IR spectra of hybrid compound, Figure S6: The HRMS spectra of hybrid compound, Figure S7: the ^1H NMR spectra of hybrid compound in CDCl_3 (500 MHz), Figure S8: the ^1H NMR spectra of hybrid compound in CDCl_3 (500 MHz), expansion in aromatic region, Figure S9: the ^1H NMR spectra of hybrid compound in CDCl_3 (500 MHz), expansion in aliphatic region, Figure S10: the 1D TOCSY spectra of aromatic region of hybrid compound in CDCl_3 (500 MHz), Figure S11: the COSY spectra of hybrid compound in CDCl_3 (500 MHz), Figure S12: the COSY spectra of hybrid compound in CDCl_3 (500 MHz), expansion in R aromatic region, Figure S13: the COSY spectra of hybrid compound in CDCl_3 (500 MHz), expansion in R'' aromatic region, Figure S14: the COSY spectra of hybrid compound in CDCl_3 (500 MHz), expansion in R''' aromatic region, Figure S15: the COSY spectra of hybrid compound in CDCl_3 (500 MHz), expansion in aliphatic region, Figure S16: the ^{13}C NMR spectra of hybrid compound in CDCl_3 (125 MHz), Figure S17: the overlay of ^{13}C NMR and DEPT-135 spectra of hybrid compound in CDCl_3 (125 MHz), Figure S18: the overlay of ^{13}C NMR and DEPT-135 spectra of hybrid compound in CDCl_3 (125 MHz), expansion in aromatic region, Figure S19: the HSQC spectra of hybrid compound in CDCl_3 (500 MHz), expansion in aromatic region, Figure S20: the ^1H - ^{13}C correlations of R aromatic region in HSQC spectra of hybrid compound in CDCl_3 , Figure S21: the ^1H - ^{13}C correlations of R'' aromatic region in HSQC spectra of hybrid compound (title compound) in CDCl_3 , Figure S22: the ^1H - ^{13}C correlations of R''' aromatic region in HSQC spectra of hybrid compound in CDCl_3 , Figure S23: the ^1H - ^{13}C correlations of aliphatic region in HSQC spectra of hybrid compound in CDCl_3 (500 MHz), Figure S24: the HMBC spectra of hybrid compound in CDCl_3 , Figure S25: the important ^1H - ^{13}C correlations of aliphatic protons in HMBC spectra of hybrid compound in CDCl_3 , Figure S26: the important ^1H - ^{13}C correlations of hydroxyl group in HMBC spectra of hybrid compound in CDCl_3 , Figure S27: the important ^1H - ^{13}C correlations of R'' and R''' aromatic protons and α , β protons in HMBC spectra of hybrid compound in CDCl_3 (a) correlation with C190.19–C159.13, (b) correlation with C144.47–C127.60, Figure S28: 3D and 2D binding poses of re-docked native ligand (4-OHT) to ER α , Figure S29: the 3D and 2D visualization of binding modes of docked compounds to ER α , (a) chalcone analogue, (b) title compound, (c) Tamoxifen, Figure S30: the visualization of MD simulation result of the title compound using Discovery Studio 2020 Client (a) 3D visualization (b) 2D visualization, Table S1: mobile phase composition for HPLC analysis of hybrid compound, Table S2: the result of docking protocol validation.

Author Contributions: Conceptualization, I.I. and R.D.; methodology, I.I., N.H., A.Z., and N.F.; software, I.I. and N.F.; synthesis work, I.I., N.H., M.M., and N.N.; in silico studies, I.I. and N.F.; Writing—Original draft preparation, I.I.; Writing—Review and editing, I.I., N.F., R.U., E.S., and N.A.; visualization, I.I.; All authors have read and agreed to the published version of the manuscript.

Funding: The in silico studies and APC were funded by Sekolah Tinggi Ilmu Farmasi Riau through grant of Penelitian Dosen Pemula with contract number of 16e.15.P3M.STIFAR.VII.2020. The synthetic work was previously funded by DRPM KEMENRISTEKDIKTI through grant of Penelitian Dosen Pemula with contract number of 06.15.LP2M.STIFAR.V.2019.

Data Availability Statement: The data presented in our study are available in the supplementary material of this article.

Acknowledgments: The authors thank DRPM KEMENRISTEKDIKTI for funding our synthesis work and Sekolah Tinggi Ilmu Farmasi Riau for funding APC and our in silico studies' work. In addition, special thanks to Lee Yean Kee, from the Department of Chemistry, Faculty of Science, University of Malaya, for sciFinder checking.

Conflicts of Interest: The authors declare no conflict of interest.

Appendix A

UV-Vis	Ultraviolet-Visible
FT-IR	Fourier Transform-Infra Red
HRMS	High Resolution Mass Spectroscopy
1D NMR	1 Dimensional Nuclear Magnetic Resonance
2D NMR	2 Dimensional Nuclear Magnetic Resonance
COSY	Correlation of Spectroscopy
TOCSY	Total Correlated Spectroscopy
HSQC	Heteronuclear Single Quantum Correlation
HMBC	Heteronuclear Multiple Bond Correlation
ER α	Estrogen Receptor Alpha
RMSD	Root Mean Square Deviation
MD	Molecular Dynamic
NPA	Nosé-Poincaré-Andersen
CHARMM27	Chemistry at Harvard Macromolecular Mechanics
4-OHT	4-Hydroxy Tamoxifen

References

- Zamri, A.; Teruna, H.Y.; Ikhtiarudin, I. The influence of power variations on selectivity of synthesis reaction of 2'-hydroxychalcone analogue under microwave irradiation. *Molekul* **2016**, *11*, 299–307. [[CrossRef](#)]
- Ikhtiarudina, I.; Agistia, N.; Frimayanti, N.; Harlianti, T.; Jasril, J. Microwave-assisted synthesis of 1-(4-hydroxyphenyl)-3-(4-methoxyphenyl)prop-2-en-1-one and its activities as an antioxidant, sunscreen, and antibacterial. *J. Kim. Sains Dan Apl.* **2020**, *23*, 51–60. [[CrossRef](#)]
- Ikhtiarudin, I.; Agistia, N.; Harlianti, T.; Zamri, A. Sintesis dan potensi aktivitas tabir surya senyawa analog kalkon turunan 3'-hidroksiasetofenon dan 4-metoksibenzaldehid. *J. Photon* **2019**, *10*, 1–12. [[CrossRef](#)]
- Syam, S.; Abdelwahab, S.I.; Al-Mamary, M.A.; Mohan, S. Synthesis of chalcones with anticancer activities. *Molecules* **2012**, *17*, 6179–6195. [[CrossRef](#)]
- Dona, R.; Frimayanti, N.; Ikhtiarudin, I.; Iskandar, B.; Maulana, F.; Silalahi, N.T. In silico, synthesis and cytotoxic activity of p-methoxy chalcone on human breast cancer MCF-7 cell line. *J. Sains Farm. Klin.* **2019**, *6*, 243–249. [[CrossRef](#)]
- Xiong, R.; He, D.; Deng, X.; Liu, J.; Lei, X.; Xie, Z.; Cao, X.; Chen, Y.; Peng, J.; Tang, G. Design, synthesis and biological evaluation of tryptamine salicylic acid derivatives as potential antitumor agents. *Med. Chem. Commun.* **2019**, *10*, 573–583. [[CrossRef](#)]
- Xu, Q.B.; Chen, X.F.; Feng, J.; Miao, J.F.; Liu, J.; Liu, F.T.; Niu, B.X.; Cai, J.Y.; Huang, C.; Zhang, Y.; et al. Design, synthesis and biological evaluation of hybrids of β -carboline and salicylic acid as potential anticancer and apoptosis inducing agents. *Sci. Rep.* **2016**, *6*, 36238. [[CrossRef](#)]
- Wang, Z.-Q.; Chang, R.-A.; Huang, H.-Y.; Wang, X.-M.; Wang, X.-Y.; Chen, L.; Ling, Y. Synthesis and biological evaluation of novel farnesylthiosalicylic acid/salicylic acid hybrids as potential anti-tumor agents. *Chin. Chem. Lett.* **2014**, *25*, 1545–1549. [[CrossRef](#)]
- Pawelczyk, A.; Sowa-Kasprzak, K.; Olender, D.; Zaprutko, L. Molecular consortia—Various structural and synthetic concepts for more effective therapeutics synthesis. *Int. J. Mol. Sci.* **2018**, *19*, 1104. [[CrossRef](#)] [[PubMed](#)]
- Shchepinov, M.S.; Case-Green, S.C.; Southern, E.M. Steric factors influencing hybridisation of nucleic acids to oligonucleotide arrays. *Nucleic Acids Res.* **1997**, *25*, 1155–1161. [[CrossRef](#)] [[PubMed](#)]

11. Urgel, J.I.; Giovannantonio, M.D.; Gandus, G.; Chen, Q.; Liu, X.; Hayashi, H.; Ruffieux, P.; Decurtins, S.; Narita, A.; Passerone, D.; et al. Overcoming steric hindrance in aryl-aryl homocoupling via on-surface copolymerization. *ChemPhysChem* **2019**, *20*, 2360–2366. [[CrossRef](#)] [[PubMed](#)]
12. Wang, Y.; Partridge, A.; Wu, Y. Improving nanoparticle-enhanced surface plasmon resonance detection of small molecules by reducing steric hindrance via molecular linkers. *Talanta* **2019**, *198*, 350–357. [[CrossRef](#)]
13. Burns, K.A.; Korach, K.S. Estrogen receptors and human disease: An update. *Arch. Toxicol.* **2012**, *86*, 1491–1504. [[CrossRef](#)]
14. Livezey, M.; Kim, J.E.; Shapiro, D.J. A new role for estrogen receptor α in cell proliferation and cancer: Activating the anticipatory unfolded protein response. *Front. Endocrinol.* **2018**, *9*, 325. [[CrossRef](#)]
15. Feng, Y.; Spezia, M.; Huang, S.; Yuan, C.; Zeng, Z.; Zhang, L.; Ji, X.; Liu, W.; Huang, B.; Luo, W.; et al. Breast cancer development and progression: Risk factors, cancer stem cells, signaling pathways, genomics, and molecular pathogenesis. *Genes Dis.* **2018**, *5*, 77–106. [[CrossRef](#)]
16. Nadji, M.; Gomez-Fernandez, C.; Ganjei-Azar, P.; Morales, A.R. Immunohistochemistry of estrogen and progesterone receptors reconsidered: Experience with 5,993 breast cancers. *Am. J. Clin. Pathol.* **2005**, *123*, 21–27. [[CrossRef](#)]
17. Sun, D.; Chen, G.; Dellinger, R.W.; Duncan, K.; Fang, J.L.; Lazarus, P. Characterization of tamoxifen and 4-hydroxytamoxifen glucuronidation by human UGT1A4 variants. *Breast Cancer Res.* **2006**, *8*, R50. [[CrossRef](#)] [[PubMed](#)]
18. Pratama, M.R.F.P.; Poerwono, H.; Siswandono, S. Design and molecular docking of novel 5-O-Benzoylpinostrobin derivatives as anti-breast cancer. *TJPS* **2019**, *43*, 201–212.
19. Prasetiawati, R.; Zamri, A.; Barliana, M.I.; Muchtaridi, M. In silico predictive for modification of chalcone with pyrazole derivatives as a novel therapeutic compound for targeted breast cancer treatment. *J. Appl. Pharm. Sci.* **2019**, *9*, 20–28.
20. Herfindo, N.; Prasetiawati, R.; Sialagan, D.; Frimayanti, N.; Zamri, A. Synthesis, antiproliferative activity and molecular docking studies of 1,3,5-triaryl pyrazole compound as estrogen α receptor inhibitor targeting MCF-7 cells line. *Molekul* **2020**, *15*, 18–25. [[CrossRef](#)]
21. Frimayanti, N.; Yaeghoobi, M.; Namavar, H.; Ikhtiarudin, I.; Afzali, M. In silico studies and biological evaluation of chalcone-based 1,5-benzothiazepines as new potential H1N1 neuraminidase inhibitors. *J. Appl. Pharm. Sci.* **2020**, *10*, 86–94. [[CrossRef](#)]
22. Jasril, J.; Ikhtiarudin, I.; Hasti, S.; Reza, A.I.; Frimayanti, N. Microwave-assisted synthesis, in silico studies and in vivo evaluation for antidiabetic activity of new brominated pyrazoline analogs. *TJPS* **2019**, *43*, 83–89.
23. Jasril, J.; Ikhtiarudin, I.; Zamri, A.; Teruna, H.Y.; Frimayanti, N. New fluorinated chalcone and pyrazoline analogs: Synthesis, docking, and molecular dynamic studies as anticancer agents. *TJPS* **2017**, *41*, 93–98.
24. Zamri, A.; Teruna, H.Y.; Wulansari, S.; Herfindo, N.; Frimayanti, N.; Ikhtiarudin, I. 3-(3,4-Dimethoxyphenyl)-5-(2-fluorophenyl)-1-phenyl-4,5-dihydro-1H-pyrazole. *Molbank* **2019**, *2019*, M1088. [[CrossRef](#)]